

ADVANCED PROBABILISTIC SIMULATION OF NPP FIRES

Simo Hostikka

VTT Building and Transport
P.O.Box 1803, FI-02044 VTT, Finland
Phone: +358 20 722 4839
E-mail: simo.hostikka@vtt.fi

Olavi Keski-Rahkonen

VTT Building and Transport
P.O.Box 1803, FI-02044 VTT, Finland
Phone: +358 20 722 4810
E-mail: olavi.keski-rahkonen@vtt.fi

ABSTRACT

The consequences of fires at NPPs can be estimated using the numerical simulation. When combined with Monte Carlo technique, the probability of target events can be calculated. The computational cost related to the use of most advanced fire models has prevented their application in this probabilistic manner. In this work, a new technique, based on an intuitive approach, is proposed. The technique allows the use of two different models in the same Monte Carlo simulation, and is therefore called Two-Model Monte Carlo (TMMC). In TMMC, simulations are first performed using both models in relatively small number of points of the random space, and the scaling functions are formed. Full Monte Carlo is then performed using the faster but less accurate model, and the results are corrected using the scaling functions. The performance of the numerical technique is studied in a simple room fire scenario, where two-zone and computational fluid dynamics (CFD) models are used. TMMC can reduce the computational cost with a factor of 30, compared to a full Monte Carlo using CFD. As a real NPP fire scenario, the distribution of component failure time is calculated in a relay room fire. In this application, CFD is used in both models but the difference in accuracy and computational cost is achieved by the refinement of the computational mesh.

Keywords: fire simulation, Monte Carlo, fire risks, electronic room, Probabilistic Fire Simulator

1 INTRODUCTION

The numerical simulation of fires can be used to estimate the consequences of prescribed fire scenarios at NPPs. When used as a part of the PSA process, the target function may be, for instance, a failure of a component of a redundant system located in the same physical space with the system catching fire. In this case, the analysis should not be limited to the most probable fire, or small group of fires as is done when using design fire concepts, but all the possible fires that can take place in the room of interest. The probability of component failure due to the fire should be calculated using Monte Carlo technique, where a large number of samples is randomly chosen from the input space and mapped through the system into the target distribution. Although Monte Carlo as a technique is almost 60 years old (Ulam 1946), its use in fire simulations has been prohibitively expensive. With modern computers the situation has changed, and the tools described here have been already applied to engineering problems. In the previous research projects concerning the fire safety of Finnish nuclear power plants, a Monte Carlo tool called Probabilistic Fire Simulator (PFS) was developed. (Hostikka & Keski-Rahkonen 2003). The tool was applied to fires in a cable tunnel and an electronics room. The tool allows the simulation of fire scenarios using various fire models, including two-zone model CFAST (Peacock et al. 1993) and Fire Dynamics Simulator (McGrattan 2004). The main outcomes of the tool are the distributions of the selected result variables, for example

component failure time, and the sensitivities of the output variables to the input variables, in terms of the rank order correlations.

The numerical simulation of the complicated physical processes is always trading between the desired accuracy of the results and the computational time required. Quite often, the same problem can be tackled by many different models with different physical and numerical simplifications. A good example of this is the fire simulation, where zone models provide a fast way to simulate the essential processes of the fire, being inevitably coarse in the physical resolution. As an alternative, computational fluid dynamics (CFD) models have higher physical resolution and can describe more complicated physical processes. On the other hand, the time needed for the computation may be longer with several orders of magnitude. A technique is therefore needed, which can combine the results of the different models in a computationally effective way. A new technique, based on an intuitive approach, is here proposed. The technique allows the use of two different models in Monte Carlo simulation, and is therefore called Two-Model Monte Carlo (TMMC). The technique is based on the assumption that the ratio of the results given by two models has smooth variations when moving from point to point of the random space. Therefore, if one of the models is presumably more accurate than the other, the ratio calculated at some point of the random space can be used to scale the result of the less accurate model in the neighbourhood of the scaling point.

In the current work, the TMMC method is first tested in a simple one room environment, where CFAST results are scaled with the FDS results, and then compared against benchmark result, obtained by performing a full Monte Carlo with FDS. The validity of the used models is not discussed here. In a realistic NPP application a relay room fire is simulated using two different FDS models. 1000 simulations are performed using a relatively coarse computational mesh, which allows fast simulations. For the scaling, 24 simulations are performed using finer computational mesh.

2 TWO-MODEL MONTE CARLO SIMULATION

During the probabilistic safety assessment process, one typically needs to estimate the probability that a certain component or system is lost during a fire. The development of fire and the response of the components under consideration are assumed to be fully deterministic processes where the same initial and boundary conditions always lead to the same final state. The probability of an event can now be calculated using Monte Carlo simulations where input variables are sampled randomly from the given distributions. Latin Hypercube sampling (McKay *et al.* 1979) is used to generate samples from all ranges of the possible values, thus giving insight into the tails of the probability distributions.

We assume that we have two numerical models A and B, that can calculate physical quantity $a(\mathbf{x},t)$ which depends on parameter \mathbf{x} and time t . In our analysis, \mathbf{x} is considered random vector from random space Ω . Model B is more accurate than model A, but the execution time of model B is longer than model A. The models are used to get two estimates of the time series: $\tilde{a}^A(\mathbf{x},t)$ and $\tilde{a}^B(\mathbf{x},t)$. The developed Two-Model Monte Carlo (TMMC) technique is based on the assumption that the results of the model A, at any point \mathbf{x} of the random space, can be made more accurate by multiplying them with scaling function, which is the ratio of model B time series to model A time series at some point \mathbf{x}_s in the vicinity of the current point \mathbf{x} . Points \mathbf{x}_s are called scaling points.

In the beginning of the simulation, the random space is divided into distinct regions. Scaling function is then calculated for each region

$$\Phi(\mathbf{x}_s, t) = \frac{\tilde{a}^B(\mathbf{x}_s, t)}{\tilde{a}^A(\mathbf{x}_s, t)} \quad (1)$$

where \mathbf{x}_s is the mid-point of the scaling region Ω_s . During the Monte Carlo, the result of model A is multiplied by the scaling function corresponding to the closest scaling point, to get the corrected times series $\tilde{a}^{AB}(\mathbf{x}, t)$

$$\tilde{a}^{AB}(\mathbf{x}, t) = \Phi(\mathbf{x}_s, t) \cdot \tilde{a}^A(\mathbf{x}, t), \quad \mathbf{x} \in \Omega_s \quad (2)$$

The result of the Monte Carlo simulation is usually not the time series itself, but some scalar property derived from

the time series. A typical result is the time to reach some critical value.

TMMC technique has been implemented in the Probabilistic Fire Simulator (PFS) tool (Hostikka & Keski-Rahkonen 2003). In practice, PFS tool is a Microsoft Excel workbook with additional function libraries for the generation of random numbers and interfacing with external fire models. Additional third-party software components are not needed in the current version of PFS.

3 RESULTS AND DISCUSSION

3.1 TMMC Validation: Simple Room Fire

The purpose of this example is to provide a realistic test for the TMMC technique. CFAST (Peacock *et al.* 1993) and FDS (McGrattan *et al.* 2004) models are used as models A and B. For the evaluation of the TMMC results, a full Monte Carlo using FDS model was first performed. Therefore, the size of the room was chosen very small in order to keep the simulation times short. The fire room was 4.0 m deep, 3.0 m wide and 3.0 m high. The room had a 1.0 m wide and 2.1 m high door to ambient. All the room boundaries were concrete and there was a concrete beam under the ceiling, 1.5 m from the back wall. The height of the beam was a random variable, ranging from zero to 0.6 m. A schematic picture of the room is shown in Fig. 1.

The fire source was a rectangular burner at the floor level. The co-ordinates and surface area of the fire source were random variables. The maximum value of the HRR per unit area was fixed to 700 kW/m². In the beginning, the heat release rate increased proportional to t^2 reaching the final value at time t_g , which was a uniformly distributed random variable. A list of the random variables is given in Table 1. The target functions were the gas temperature and activation time of a heat detector under the room ceiling, left from the concrete beam. For gas temperature, the time to reach 200 °C was monitored.

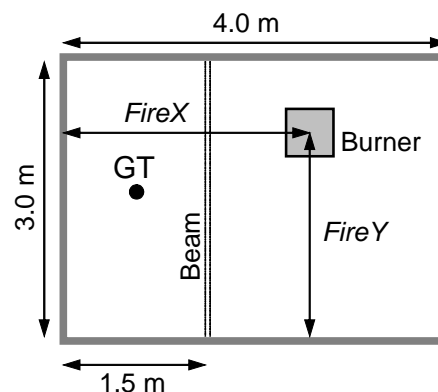


Fig. 1. The geometry of the room fire scenario. GT shows the location of the heat detector and the gas temperature measurement point 5 cm under the ceiling.

The absolute accuracy of the fire simulation codes is not discussed here. It was simply assumed, that FDS results were more accurate than CFAST results. In CFAST, two virtual rooms were used by splitting the room at the beam location. In FDS, the room was divided into control volumes with a side length of 0.10 m. Before the actual TMMC application, simulations using only CFAST and only FDS were carried out. With one thousand iterations for both models, the final distributions were well converged. The maximum difference between the cumulative distributions after 500 iterations and 1000 iterations was 0.015 (1.5 %). The difference was smallest in the tails of the distributions, being order of 0.001 (0.1 %).

Table 1. A list of random variables in the room fire example.

Variable	Units	Distribution type	Min	Max	Mean	Std.dev
BeamHeight z_B	m	Uniform	0.0	0.6		
GrowthTime t_g	s	Uniform	60	180		
FireArea	m ²	Normal	0.2	1.50	0.80	0.60
FireX	m	Uniform	0.0	4.0		
FireY	m	Uniform	0.0	3.0		

The effect of the number of TMMC scaling points was studied by using different ways to divide the random

space. The number of scaling points varied from one to 32. A summary of the different versions is given in Table 2. The basis for the division was taken from the CFAST simulations, which predicted that the fire surface area, HRR growth time and FireX-position were the important random variables. Due to the division to the virtual rooms, FireX variable was especially interesting as the results had a clear discontinuity at FireX = 1.5 m. Therefore, more divisions were used for FireX than other variables in some of the cases.

A comparison of predicted probability distributions for the time when gas temperature reaches 200 °C is shown in Fig. 2. The large difference in the distributions of CFAST and FDS codes made this a challenging problem for TMMC scaling. The overall probability was 63.5 % according to CFAST, while FDS results lead to a final probability of 90.70 %. Unfortunately, the simulation time was slightly too short for FDS distribution to reach a fully converged value. Therefore, an uncertainty of 1 % percentage unit is associated with the final probability given by FDS.

Table 2. A summary of scaling divisions in different TMMC versions.

Name	N_{tot}	$N(z_B)$	$N(t_g)$	$N(Area)$	$N(FireX)$	$N(FireY)$
TMMC(1)	1	1	1	1	1	1
TMMC(3)	3	1	1	1	3	1
TMMC(6)	6	1	2	1	3	1
TMMC(27)	27	1	3	3	3	1
TMMC(32)	32	1	4	4	2	1
TMMC(32B)	32	2	2	2	2	2

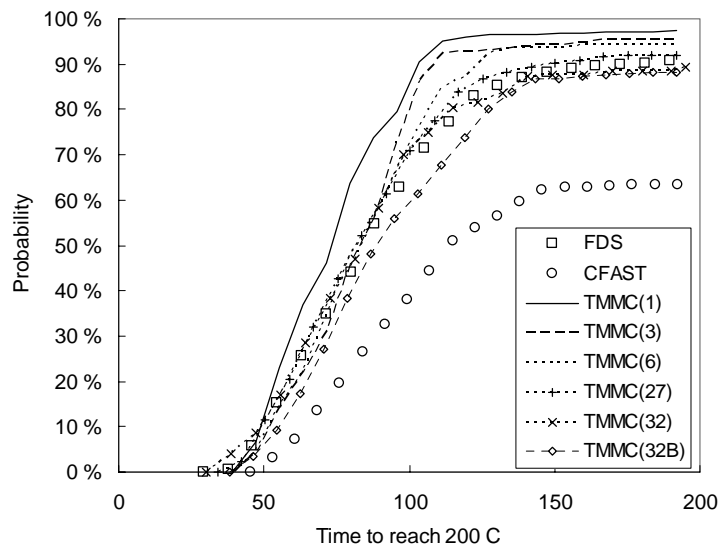


Fig. 2. A comparison of predicted probability distributions of time to reach 200 °C.

The division of the random space had a clear effect on the accuracy of the TMMC distribution. If the division was made based on the information of the relative importance of the random variables, the higher number of scaling points generally improved the accuracy. However, if the scaling points were chosen without prior information of the importance, the results did not improve as much as one might have expected, as was shown in the case TMMC(32B). In addition to this effect, the smoothness of the transient data affected the quality of the results. This is demonstrated in Fig. 3 that shows the errors in the final probability in two cases. In the upper curve, the FDS data was not smoothed before the calculation of the scaling function $\Phi(x_s, t)$ and in the lower curve a 5-point running average was taken. The original FDS data was saved with 2.0 second intervals. In the case of 32 scaling points, the smoothed FDS data, which mostly works better, gave higher error than the original. The reason for this is currently not known. However, the smoothing had here a strong effect because the target function was

the gas temperature. In practical applications, the target function is usually temperature of some solid object. Such an object has some thermal inertia which automatically smoothes out the fluctuations of the temperature field, and the post-processing smoothing discussed here may not be needed.

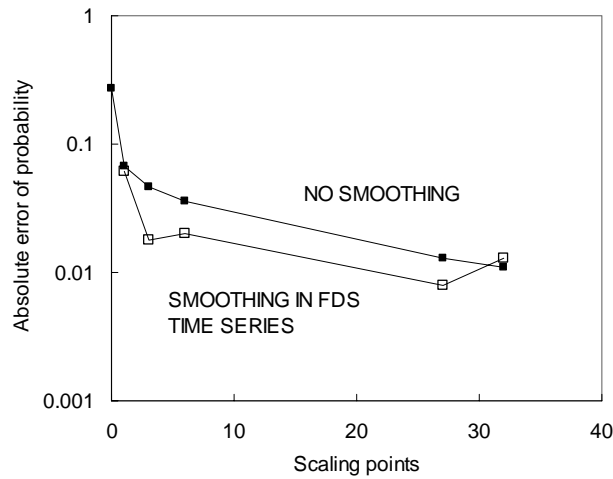


Fig. 3. The accuracy of predicted final probability as a function of number of scaling points.

The effect of end probability on the accuracy of the TMMC scaling was studied by varying the critical gas temperature from 150 °C to 500 °C. In Fig. 4, the predicted end probabilities are shown as a function of the probability given by FDS. The lowest probabilities correspond to the highest values of the critical gas temperature. The correct result is at the diagonal of the figure. TMMC probabilities corresponding to 6, 27 and 32 scaling points are very close to the diagonal but the uniform distribution of scaling points (case 32B) results in clearly lower probabilities. An important observation of the figure is that, while CFAST did not observe the highest temperatures at all, after the scaling these highest temperatures are found, leading to non-zero probabilities in the low left corner of the figure. The accuracy of the smallest probabilities is sensitive to the smoothing of the FDS data. Here, the FDS results were obtained from the "raw" data without any smoothing, but 5 point smoothing was used before the computation of the scaling functions.

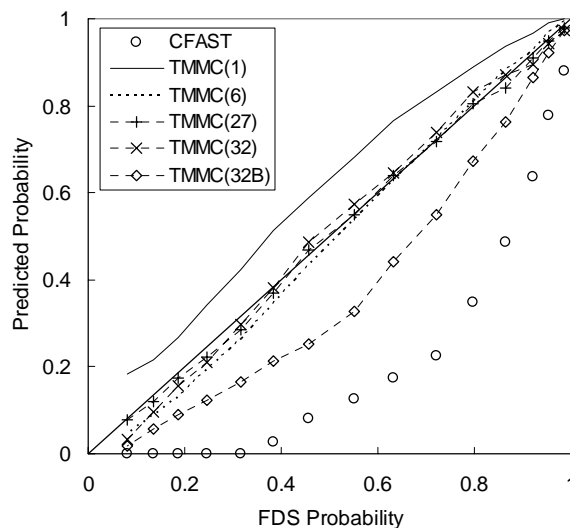


Fig. 4. The effect of the final probability on the TMMC accuracy.

TMMC scaling was also found to improve the predicted sensitivity measures. Fig. 5 shows the predicted Spearman's rank order correlation coefficients between the time to reach 200 °C temperature and the random

variables. For most variables all three methods, CFAST, FDS and TMMC, gave very similar coefficients. However, for the HRR growth time CFAST gave much lower RCC than FDS, but TMMC result was very close to FDS result. The case with 27 scaling points was used.

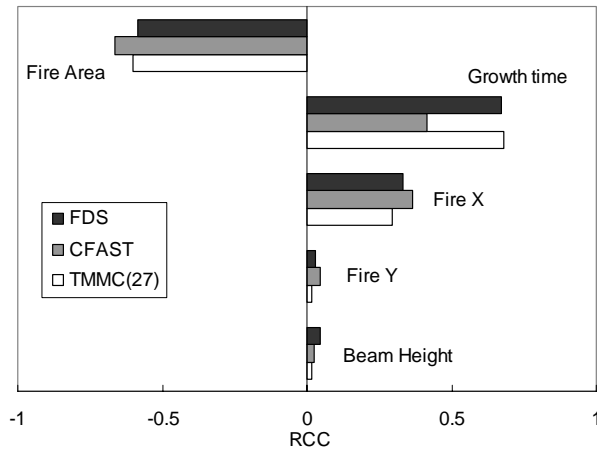


Fig. 5. Rank order correlation coefficients for the gas temperature reaching time.

3.2 NPP Relay Room Fire

A fire in a relay room containing about 200 electronics cabinets filled with relays, circuit boards and cables is studied. The room contains cabinets of two redundant sub systems separated by physical distance. The target of the simulation is the time dependent component failure probability of the second sub system, when the fire ignites in a cabinet being part of the first sub system. Once ignited, the fire heats up the neighboring cabinets being in the direct contact with the ignition cabinet. The smoke flows out of the cabinet through the ceiling vent, fills the room and possibly activates the smoke detectors. The geometry of the room is illustrated in Fig. 6. All the room walls, floor and ceiling are made of concrete, and the ceiling is supported by 0.40 m high concrete beams with 3.0 m spacing, as shown in Fig. 6. The ceiling height is 3.0 m. All the doors to the room are assumed to be closed. The room is equipped with smoke detectors placed in the ceiling.

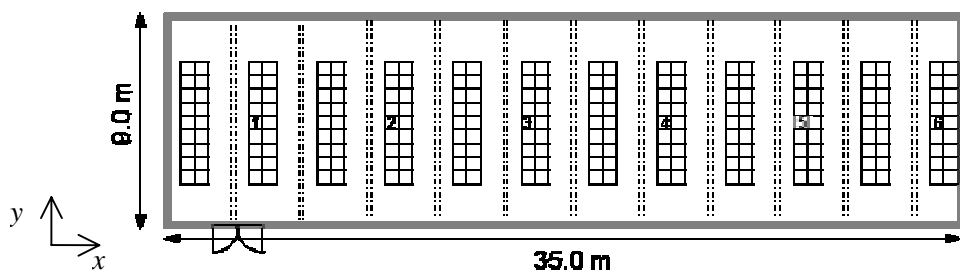


Fig. 6. Plan view of the relay room, with approximate locations of the cabinets and concrete beams. The numbers from 1 to 5 indicate the ignition locations.

The volumetric flow of the mechanical ventilation is $4 \text{ m}^3/\text{s}$. The ventilators are oriented vertically, and located below the concrete beams supporting the ceiling. The incoming air temperature is normally $18\text{--}20 \text{ }^\circ\text{C}$. Temperature is controlled by air cooling and moisturizing unit. When a fire is detected in the room, the ventilation system is automatically closed from the other ventilation systems of the building and room air is circulated from room via cooling unit back to the room. The power of the cooler is 48 kW. The electronics cabinets are rectangular, vertical boxes with walls and ceiling made of 1.0 mm thick steel plates and concrete floor. The cabinets have openings at the bottom and top for natural ventilation. The material properties of the cabinet steel are shown in Table 3.

The fire starts inside one of the cabinets. Based on the earlier studies, it is known that the spreading of the fire inside the ignition cabinet determines the conditions in the room in the early phases of the fire, and acts as a boundary condition for the further spreading of the fire. Due to the high uncertainty associated with the numerical

flame spread predictions, the development of this early fire is described by simple analytical model where the heat release rate (HRR) increases as a t^2 -type curve until it reaches a maximum level, which depends on the geometry of the cabinet. In this work, the growth rate and the maximum HRR are random variables with uniform distributions based on the earlier analytical and experimental information (Mangs & Keski-Rahkonen 1996). The total combustible mass per cabinet determines the overall burning time and is treated as a random variable. In addition to the parameters of the heat release rate curve, the location of the ignition cabinet is also chosen randomly. Six possible locations in x -direction, i.e. six rows are considered. These rows are shown with numbers 1...6 in Fig. 6.. The y -location inside the row (column) is also chosen randomly.

Table 3. Material properties in the relay room simulation.

	Combustible PVC	Concrete	Steel plate	Target plastic
Thermal Model	Thick charring	Thick	Thin	Thick
Density (kg/m ³)	1300	2100	7850	1300.
Conductivity (W/m.K)	0.16	1.0		0.16
Specific heat (J/kg.K)	1500	880	460	1500
Char density (kg/m ³)	400			
Moisture fraction	0.1			
Heat of vaporization (J/kg)	2.0·10 ⁶			
Heat of combustion (J/kg)	2.1·10 ⁷			
Ignition temperature (°C)	Random			
Char conductivity (W/m.K)	0.1 ... 0.3 (*)			
Char specific heat (J/kg.K)	1000... 100. (*)			

*) Temperature-dependent properties.

The ignition cabinet is directly connected to two or three neighboring cabinets. The fire may spread to the neighboring cabinets by heating up the cable materials inside the neighbors. In this special case, a fire spreading from one cabinet to its neighbor cabinet is not very interesting from plant's probabilistic risk assessment point of view, because all the neighboring cabinets are members of the same sub system. However, the spreading of the fire to neighboring cabinets in a row increases the heat release rate, and may therefore have considerable effect on the failure probability in the next row. For the modeling of the fire spread inside the cabinet row, all the cabinets of the row are filled with combustible PVC-material. The total combustible mass within the neighboring cabinets is the same as the ignition cabinet. The material properties are given in Table 3. Each cabinet contains 2.5 m² of thin (4 mm) thick PVC-board and 0.64 m² of thick board accounting the rest of the combustible mass. In preliminary simulations, it was found that FDS can qualitatively predict the flame spread inside the cabinet. Physically, the neighboring cabinets are identical to the ignition cabinet. The spreading of fire to other cabinet rows is not studied.

The main purpose of the simulations is to find the probability of component failure in the adjacent cabinet row belonging to another sub system. The physical construction of the adjacent cabinets is the same as the ignition cabinet. To model the heating of the most sensitive components of the target cabinets, a 2 mm thick plastic board was placed inside the target cabinets, and the temperature of the plastic board was solved and monitored. The material properties of the boards are shown in Table 3.

The simulations were performed with Fire Dynamics Simulator (FDS) version 4.01 (McGrattan 2004). An overview of the FDS model of the relay room is shown in Fig. 7. The spatial discretization is summarized in Table 4. Four different zones of the room are defined with different grid cell sizes: Ignition cabinets' zone covers the cabinet row containing the ignition source. The room space outside the ignition cabinets is divided to lower part and upper part. The upper part covers the space above the cabinets. In this application, FDS model is used in both phases of TMMC: Model A is a FDS model with relatively coarse computational mesh and Model B is FDS with fine computational mesh. 1000 simulations were performed using model A and 24 simulations using model B. The distribution of TMMC scaling points is shown in Table 5. Each simulation of model A took about 24 h on one CPU of modern workstation. The model B simulations took about 5 days each. The simulations were performed on a group of 8 workstations with 2 CPUs on each computer. Figures 8 and 9 show some examples of the simulation results. In Fig. 8, the gas temperature field at height 2.40 m at time = 700 s after the ignition is presented. The effect of the ventilation can be seen on the left side of the room, where fresh air is blown into the room from the air channels. The vertical temperature distribution inside and above the ignition cabinet, also at time 700 s, is shown in Fig. 9. The neighboring cabinet has just ignited and the fire is spreading downwards on the surfaces of the

PVC-boards.

Table 4. Cell sizes of the coarse and fine FDS models in relay room scenario.

Zone of the room	Cell size (m)	
	Coarse model (A)	Fine model (B)
Ignition cabinets	0.10	0.05
Room, lower part	0.30	0.20
Room, upper part	0.30	0.10
Air channel	0.20	0.20

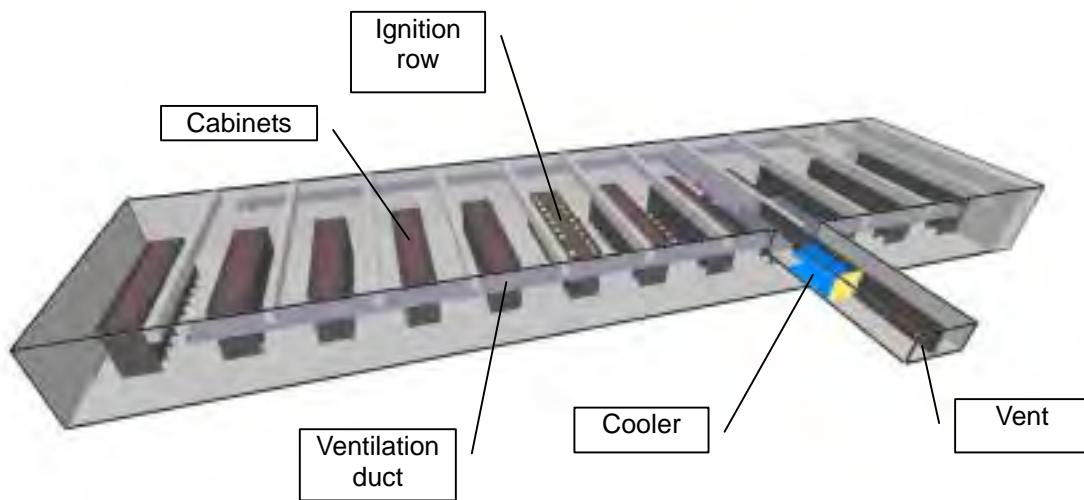


Fig. 7. An overview of the FDS model of the relay room.

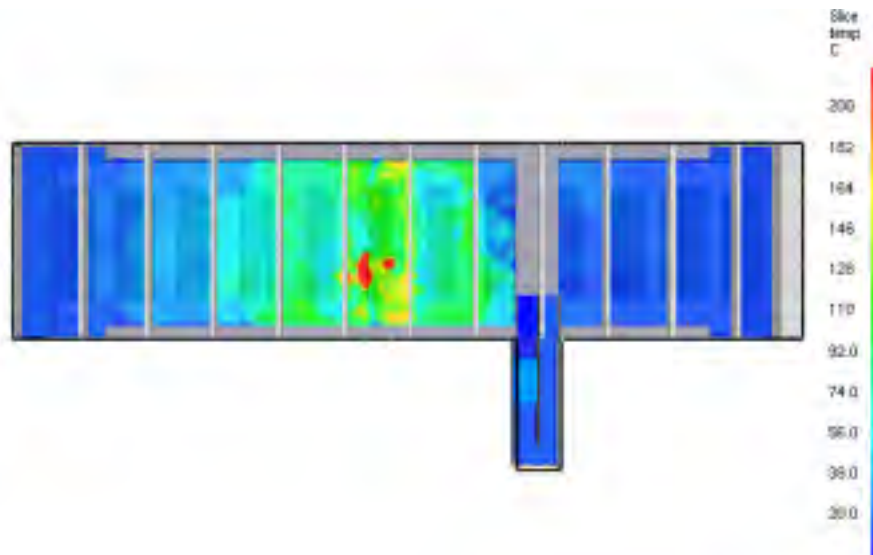


Fig. 8. Instantaneous temperature at height $z = 2.4$ m, 700 s after the ignition.

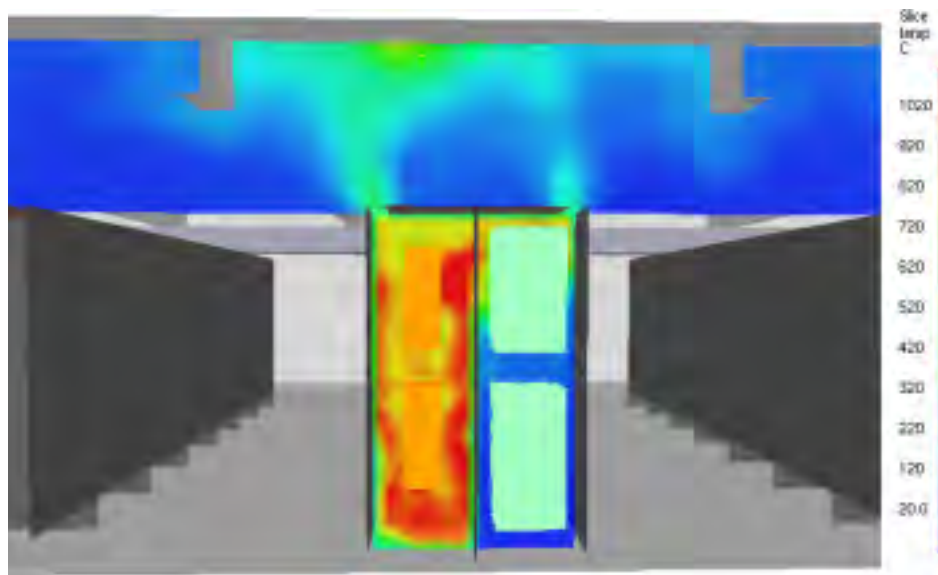


Fig. 9. Instantaneous temperature inside and above the cabinets, 700 s after the ignition.

A list of random variables is shown in Table 5. HRR Growth rate is the growth time coefficient of the ignition cabinet HRR curve. Row number and Column number define the location of the ignition cabinet inside the room. Combustible mass is the mass of circuit boards and cables inside the ignition cabinet. Cooler power is varied to find out the importance of the room cooling. The uncertainty related to the material properties of the cabinet contents is described as the variation of the ignition temperature. This feature is only applied to the ignition of the neighboring cabinets. The maximum HRR of the ignition cabinet is varied in accordance to the variation of the available experimental data (Mangs & Keski-Rahkonen 1996, Hostikka & Keski-Rahkonen 2003).

The failure times of the critical components were calculated for three different critical temperatures: 80 °C, 100 °C and 120 °C. For the calculation, the target temperature was chosen to be the maximum of the cabinets in both neighboring rows. The cumulative distributions of the failure times are shown in Fig. 10. The final probabilities corresponding to the three critical temperatures are 0.41, 0.091 and 0.006. The average values of the failure times are 23, 24 and 25 minutes. The uncertainty of the probability curves comes from both the statistical uncertainty and the uncertainty of the physical modeling. Here, the modeling uncertainty is the dominating source of error. An estimate for the uncertainty of the given probabilities is ± 0.1 .

Table 5. List of random variables in the relay room scenario.

Variable	Distribution type	Mean	Min	Max	Units	N_{TMMC}
HRR Growth time	Uniform(750,2000)	1375	750	2000	s	3
Row number	Discrete(1,2,3,4,5,6)					1
Column number	Discrete(1,2,3,4,5,6,7,8,9)					1
Combustible mass	Uniform(20,60)	40	20	60	kg	2
Cooler power	Uniform(0,96)	48	0	96	kW	1
Ignition temperature	Uniform(310,350)	330	310	350	°C	2
Maximum HRR of a cabinet	Uniform(200,450)	325	200	450	kW	2

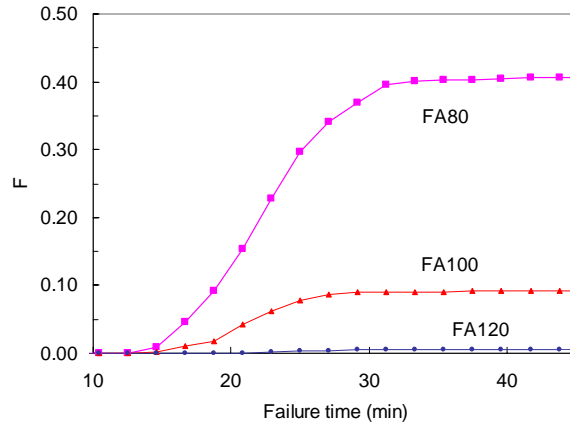


Fig. 10. Cumulative distribution of the target failure times. The three curves correspond to critical temperatures 80, 100 and 120 °C.

The sensitivity of the failure time FA80 to the input variables was studied by calculating the rank order correlations (ROC), shown in Fig. 11. As can be seen, the HRR growth time is the dominating input. All the other inputs have much smaller effects. The physical location in the room seems to have some effect, possibly due to the asymmetric ventilation conditions.

At the time of the simulations, FDS model did not have a model for the smoke detector actuation. Therefore, the activation of the smoke detectors in the ceiling of the room was studied by using heat detectors with very low activation temperatures, which is a standard technique in fire simulation. To account for the uncertainty of the method, three different activation temperatures were used: 23 °C, 26 °C and 29 °C. The initial temperature of the room was 20 °C. The RTI parameter defining the thermal inertia of the detectors was 50 (m.s)^{1/2}. In addition to the heat detectors, the activation of the possible sprinkler system was studied by placing a sprinkler head with activation temperature of 68 °C above the fire. The sprinkler was not used for fire suppression, though. The cumulative distributions of the heat detector and sprinkler activation times are shown in Fig. 12. Considerable differences are found in the detection times corresponding to the three detection temperatures. While 50 % of the HD23 events have taken place after 2.5 minutes, more than 8 minutes are needed to have 50 % of the HD29 events. This result demonstrates that the simulation of smoke detector activation may be very sensitive to the selected temperature.

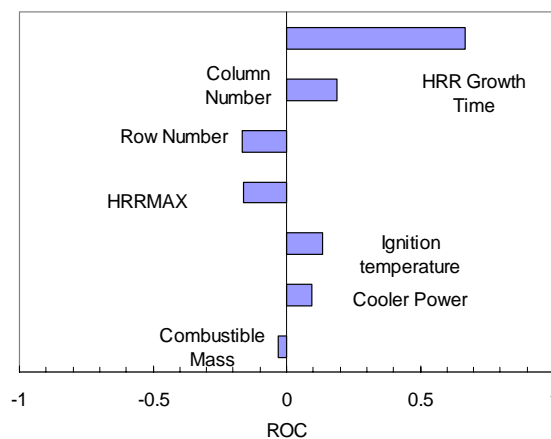


Fig. 11. Sensitivity of the failure time (FA80) to the inputs.

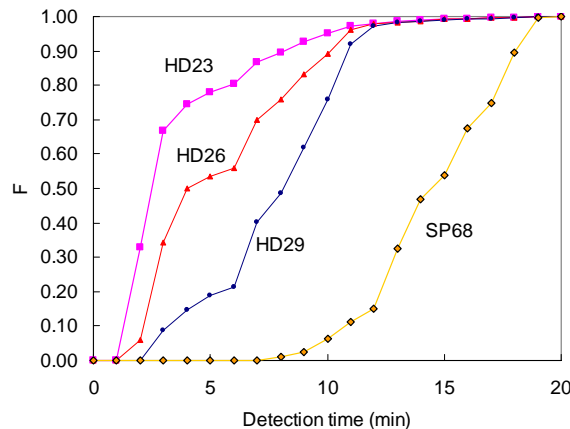


Fig. 12. Cumulative distribution of fire detection times. Curves HD23, HD26 and HD29 correspond to the heat detectors with activation temperatures of 23 °C, 26 °C and °C, respectively. SP68 is a sprinkler head

The manual fire fighting procedures was not included in the simulations. However, the probability of successful fire fighting can be estimated by calculating the available operation time of the fire fighters by subtracting the detection time (HD26) from the failure time (FA80). The distribution of the available operation time is shown in Fig. 13. The average available operation time is 16.7 min. In 2.67 % of the fires, the available time is less than 10 min. A closer look at the simulation results data showed that the smallest available operation times are caused by the late fire detection, not early failure. The fire fighters' ability to find the fire source is strongly affected by the loss of visibility in smoke. The time of losing visibility was calculated by monitoring the visibility at the room entrance door and saving the time when the visibility reached a value of 1.0 m. In Fig. 13, also the distribution of the available visible time is shown. It is clear, that the fire fighters will have difficulties finding the fire source unless they can enter the room within six minutes from the fire detection.

Another factor affecting the fire fighters ability to suppress the fire is the fire size. The distributions of the total heat release rate (HRR) at the time of failure (FA80) and the maximum HRR values of are shown in Fig. 14. The highest observed HRR values are about 10 MW corresponding to a fire of the whole row of cabinets. Despite the possible uncertainties associated with the distributions of the total HRR, it is clear that the fire fighters will have to deal with a fire covering several cabinets.

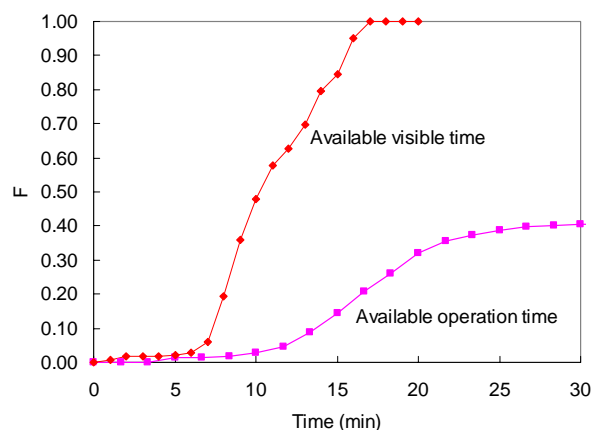


Fig. 13. Cumulative distributions of the available operation time and available visible time.

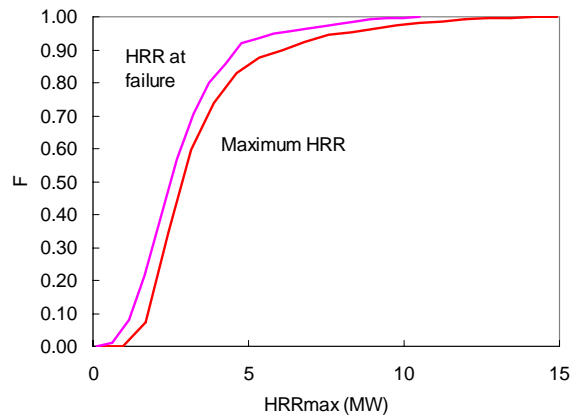


Fig. 14. Cumulative distributions of the heat release rate (HRR) at the time of the failure (FA80) and maximum HRR over the whole fire duration.

4 CONCLUDING REMARKS

Probabilistic Fire Simulator is a tool for Monte Carlo simulations of fire scenarios. The tool is implemented as a worksheet computing tool, and can be used as user interface for various fire models. The Monte Carlo simulations can provide the distributions of the output variables and their sensitivities to the input variables. Typical outputs are for example the times of component failure, fire detection and flashover.

The computational cost of the advanced fire simulation codes often prevents their application in Monte Carlo simulation. In practical simulations, zone models or CFD models with very coarse computational mesh must be used. A new technique is here proposed for the improvement of the accuracy of the simple fire models. Two-Model Monte Carlo is a computationally affordable technique to utilize advanced simulation techniques like CFD in the probabilistic safety assessment of large systems. The results of the simple but inaccurate simulation models can be corrected by scaling them with the results achieved from an order of few tens of simulations with the more advanced model. Good accuracy can be achieved if the existing information on the relative importance of the random variables is used to efficiently place the scaling points. If such information is not available, or is not reliable, the random space must be divided uniformly in all dimensions, and the number of required scaling points may become very high.

The presented application demonstrates the use TMMC technique to a NPP relay room fire. Realistic distribution of the failure times of critical components were found and the distribution of available operation time for the fire fighters was estimated by combining the failure time and fire detection information.

ACKNOWLEDGEMENTS

The authors wish to thank Dr. Timo Korhonen of VTT for his contribution in the PFS development and data collection. This study has been financed by the Finnish Centre for Radiation and Nuclear Safety, the Ministry of Trade and Industry, Fortum Engineering Ltd. and TeollisuudenVoima Oy.

REFERENCES

- Hostikka, S. & Keski-Rahkonen, O. (2003) Probabilistic simulation of fire scenarios. Nuclear engineering and design., vol. 224 (2003) 3, pp. 301-311.
- Mangs, J. & Keski-Rahkonen, O. 1996. Full scale fire experiments on electronic cabinets II. Espoo, Technical Research Centre of Finland. 1996. 48 p. + app. 6 p. VTT Publications 269
- McGrattan, K. (ed.) 2004. Fire Dynamics Simulator (Version 4) - Technical Reference Guide. National Institute of Standards and Technology, Gaithersburg, MD. Special Publication 1018. 94 p.

McKay, M.D., Beckman, R.J. & Conover, W.J. (1979) A comparison of three methods for selecting values of input variables in the analysis of output from a computer code. *Technometrics*, 21(2). pp. 239-245.

Peacock, R.D., Forney, G.P., Reneke, P., Portier, R. & Jones, W.W. (1993) CFAST, the Consolidated Model of Fire Growth and Smoke Transport. Gaithersburg, National Institute of Standards and Technology, NIST Technical Note 1299. 118 p. + app. 116 p.

Ulam, S.M., 1946, as quoted in: <http://www-gap.dcs.st-and.ac.uk/~history/Mathematicians/Ulam.html> and <http://members.aol.com/jeff570/mathword.html>.